Methotrexate enhances the antianabolic and antiproliferative effects of 5-aminoimidazole-4-carboxamide riboside

Annelies Beckers,[1] Sophie Organe,[1] Leen Timmermans,[1] Frank Vanderhoydonc,[1] Ludo Deboel,[1] Rita Derua,[2,3] Etienne Waelkens,[2,3] Koen Brusselmans,[1] Guido Verhoeven,[1] and Johannes V. Swinnen[1]

[1]Laboratory for Experimental Medicine and Endocrinology, [2]Division of Biochemistry, and [3]BioMacs and ProMeta, Katholieke Universiteit Leuven, Leuven, Belgium

Abstract

Because of its ability to mimic a low energy status of the cell, the cell-permeable nucleoside 5-aminoimidazole-4-carboxamide (AICA) riboside was proposed as an antineoplastic agent switching off major energy-consuming processes associated with the malignant phenotype (lipid production, DNA synthesis, cell proliferation, cell migration, etc.). Key to the antineoplastic action of AICA riboside is its conversion to ZMP, an AMP mimetic that at high concentrations activates the AMP-activated protein kinase (AMPK). Here, in an attempt to increase the efficacy of AICA riboside, we pretreated cancer cells with methotrexate, an antimetabolite blocking the metabolism of ZMP. Methotrexate enhanced the AICA riboside–induced accumulation of ZMP and led to a decrease in the levels of ATP, which functions as an intrasteric inhibitor of AMPK. Consequently, methotrexate markedly sensitized AMPK for activation by AICA riboside and potentiated the inhibitory effects of AICA riboside on tumor-associated processes. As cotreatment elicited antiproliferative effects already at concentrations of compounds that were only marginally effective when used alone, our findings on the cooperation between methotrexate and AICA riboside provide new opportunities both for the application of classic antimetabolic chemotherapeutics, such as methotrexate, and for the exploitation of the energy-sensing machinery as a target for cancer intervention. [Mol Cancer Ther 2006;5(9):2211–7]

Introduction

Malignant cells typically show a high rate of anabolic processes. They frequently overexpress lipogenic enzymes, such as fatty acid synthase, show enhanced protein biosynthesis, and are more active in synthesizing DNA. All these processes require energy; hence, interference with the cellular mechanisms governing energy homeostasis was proposed recently as a novel strategy in the battle against cancer (1–3). Key target in this strategy is the AMP-activated protein kinase (AMPK), a cellular fuel gauge that is exquisitely sensitive to changes in the levels of the low energy indicator AMP (4–6). On binding of AMP, AMPK phosphorylates several downstream targets, including key anabolic enzymes, inhibiting their activity and this way switching off major energy consuming pathways. In a recent attempt to explore the feasibility of targeting the energy sensing system as a strategy in the treatment of cancer, cancer cells were treated with 5-aminoimidazole-4-carboxamide (AICA) riboside, a cell-permeable nucleoside (1–3). On cell entry, AICA riboside is phosphorylated by adenosine kinase to AICA ribotide, also known as ZMP, which mimics the effects of AMP in activating AMPK (6, 7). In cultures of cancer cells, the AICA riboside–induced increase of ZMP levels blocks tumor-associated anabolism, attenuates tumor cell proliferation, impedes cell invasiveness, and inhibits the ability of cancer cells to form colonies (1–3). One important shortcoming of AICA riboside is the large amount of drug that is needed to exert effects. This problem is related in part to the rapid metabolism of ZMP entering into the *de novo* purine synthesis pathway (8) and to the inhibitory influence of ATP on the activation of AMPK (9). Here, reasoning that these limitations could be overcome by inhibition of the *de novo* purine synthesis, we cotreated cancer cells with AICA riboside and methotrexate (4-amino-10-methylpteroylglutamic acid). Methotrexate is an antimetabolite that already for several decades is being used clinically in the treatment of a variety of malignancies (10). It exerts cytotoxic effects through direct inhibition of dihydrofolate reductase and inactivation of folate-dependent enzymes, including glycinamide ribonucleotide transformylase (GART) and AICA ribotide transformylase/IMP cyclohydrolase (ATIC), two key enzymes of the *de novo* purine biosynthesis pathway, responsible for

Received 1/3/06; revised 6/6/06; accepted 6/29/06.

Grant support: Fortis Bank Insurance and VIVA; Concerted Research Action Fund (Katholieke Universiteit Leuven); Fund for Scientific Research-Flanders research grants (Belgium; F.W.O.); and Interuniversity Poles of Attraction Programme-Belgian State, Prime Minister's Office, Federal Office for Scientific, Technical, and Cultural Affairs grant.

The costs of publication of this article were defrayed in part by the payment of page charges. This article must therefore be hereby marked advertisement in accordance with 18 U.S.C. Section 1734 solely to indicate this fact.

Note: L. Timmermans and K. Brusselmans are research assistant and postdoctoral fellow, respectively, of the Fund for Scientific Research-Flanders (Belgium).

Requests for reprints: Johannes V. Swinnen, Laboratory for Experimental Medicine and Endocrinology, Katholieke Universiteit Leuven, Gasthuisberg, O&N, Herestraat 49 bus 902, B-3000, Leuven, Belgium. Phone: 32-16-34-59-70; Fax: 32-16-34-59-34. E-mail: johan.swinnen@med.kuleuven.be

doi:10.1158/1535-7163.MCT-06-0001

the conversion of glycinamide ribonucleotide to formylglycinamide ribonucleotide and of ZMP to IMP, respectively, in the final steps of the *de novo* purine synthesis (11, 12). The major inhibitory effect of methotrexate is due to depletion of 10-formyltetrahydrofolate, the one-carbon donor for both of these reactions. In addition, methotrexate polyglutamate derivatives that accumulate in cells are the direct inhibitors of both ATIC and GART, but they most potently inhibit ATIC (13–15). The net result is an inhibition of the *de novo* purine biosynthesis leading to a depletion of ATP and to a lesser extent of GTP (15, 16). In contrast to normal cells, which prefer the purine salvage pathway, rapidly dividing tumor cells rely on the *de novo* pathways explaining part of the chemotherapeutic action of methotrexate. Here, we show that methotrexate, by blocking the *de novo* purine biosynthesis pathway, enhances the ability of exogenous AICA riboside to increase the levels of ZMP and leads to a decrease in the levels of ATP. Consequently, methotrexate sensitizes AMPK for activation by AICA riboside and enhances the AICA riboside–induced inhibition of tumor-associated anabolism and colony formation.

Materials and Methods

Cell Culture

MDA-MB-231 and A-431 cells were obtained from the American Type Culture Collection (Manassas, VA) and maintained at 37° C in a humidified incubator with a 5% CO_2/95% air atmosphere (MDA-MB-231) or a 10% CO_2/90% air atmosphere (A-431) in RPMI 1640 (MDA-MB-231) or DMEM (A-431) supplemented with 10% FCS (Invitrogen, Carlsbad, CA). PC-3M-luc-C6 cells were obtained from Xenogen Corp. (Alameda, CA). These cells were maintained at 37°C in a 5% CO_2/95% air atmosphere in MEM supplemented with 10% FCS, 1% sodium pyruvate (Invitrogen), 1% MEM vitamin solution (Invitrogen), and 1% MEM nonessential amino acids (Invitrogen).

Preparation of Methotrexate-Albumin

Methotrexate and albumin were purchased from Sigma (St. Louis, MO). Methotrexate-albumin was prepared as described by Stehle et al. (17).

Measurement of ZMP and ATP

Cells were plated on day 0. On day 1, they were treated with methotrexate, methotrexate-albumin, or vehicle. One day later, cultures received different concentrations of AICA riboside. After 2 hours of incubation, cultures were washed twice with PBS, harvested, and centrifuged. ZMP was measured by quantification of the m/z 127 product ion by tandem mass spectrometry on a Finnigan LTQ Linear Ion Trap mass spectrometer (Thermo Electron Corporations, San Jose, CA). ATP levels were determined using the luciferase/luciferin-based ENLITEN ATP assay system (Promega, Madison, WI).

Immunoblot Analysis

Cells treated with different concentrations of methotrexate, methotrexate-albumin, and/or AICA riboside were washed with PBS and lysed in a reducing NuPage sample loading buffer (Invitrogen). Equal amounts of protein were separated on NuPage gels (Invitrogen) and processed for immunoblot analysis for AMPKα, phosphorylated Thr^{172} AMPKα, phosphorylated Ser^{79} acetyl-CoA carboxylase, and cytokeratin-18 as described (1).

Incorporation of 2-[^{14}C]Acetate into Cellular Lipids

Cells were treated with methotrexate, methotrexate-albumin, and/or AICA riboside as indicated. One hour after addition of AICA riboside (or vehicle), 2-[^{14}C]-labeled acetate (2 μCi/6-cm dish; 57 mCi/mmol; Amersham Biosciences, Piscataway, NJ) was added to the cultures. Four hours later, cells were washed with PBS, scraped, and resuspended in 0.9 mL PBS. Lipids were extracted using the Bligh-Dyer method as described previously (18). Incorporation of ^{14}C into lipids was measured by scintillation counting.

Analysis of DNA Synthesis

Cells were treated with methotrexate, methotrexate-albumin, and/or AICA riboside as described. DNA synthesis was measured using the bromodeoxyuridine (BrdUrd) labeling and detection kit III (Roche Applied Science, Hague Road, IN).

Determination of Synergism

The combination index (CI) method of Chou and Talalay (19) was used to analyze the nature of the pharmacologic interaction between methotrexate and AICA riboside. Synergism is defined as more than the expected additive effect with $CI < 1$, whereas $CI > 1$ indicates antagonism (19, 20).

Colony Formation Assay

Cells were seeded at a density of 5×10^3 per 6-cm dish and treated as indicated. Eight days after initial treatment, cultures were fixed with 4% formaldehyde in PBS and stained with a 0.5% crystal violet solution in 25% methanol. Plates were photographed with a Nikon Coolpix digital camera (Nikon Corp., Tokyo, Japan).

RNA Interference

The day before transfection, cells were plated at a density of 5×10^5 per 6-cm dish. Transfection of cells with Stealth small interfering RNA (siRNA) using LipofectAMINE 2000 (Invitrogen) was carried out according to the manufacturer's protocol. Stealth siRNA molecules targeting ATIC (5′-CCUGCAAUCUCUAUCCCUUUGUAAA-3′) and GART (5′-GGCAGCUGGAGAAACAAUUGUCAUU-3′) and a nonspecific control double-stranded RNA, designed by scrambling the nucleotide sequence of the ATIC siRNA (5′-CCUAACUCUAUCUCCUUGUUGGAAA-3′), were purchased from Invitrogen. Twenty-four hours after transfection, cells were trypsinized and reseeded at a density of 5×10^3 per dish for colony formation assay.

RNA Analysis

A 556-bp cDNA probe for ATIC and a 620-bp cDNA probe for GART were synthesized by PCR on human cDNA (generated by reverse transcription as described previously; ref. 15). For the ATIC probe, the primers were 5′-CCAGCTGTACACACTGCAGCC-3′ (forward) and 5′-TTATGACTTGTCGACGACACC-3′ (reverse). The GART probe was synthesized using 5′-AGGCTCAAGCTCTAGGACTGG-3′ and 5′-TCCAAGGAGAGCACATCCAGC-3′ as forward and reverse primer, respectively. Probes for 18S

rRNA, RNA preparation, and Northern blot procedures have been described previously (21).

Statistics

Statistical analyses were done using one-way ANOVA with Tukey's multiple comparison test.

Results

Methotrexate Enhances the Ability of AICA Riboside to Activate AMPK by Stimulating the Accumulation of ZMP and by Decreasing the Levels of ATP

To examine the ability of methotrexate to enhance the effects of AICA riboside, three human cancer cell lines were used, MDA-MB-231 breast cancer cells, PC-3M-luc-C6 prostate cancer cells, and A-431 epidermoid carcinoma cells. MDA-MB-231 cells are the most thoroughly characterized in terms of their response to AICA riboside (1). Like many clinical cancers, they are resistant to native methotrexate due to transport deficiencies caused by an epigenetic alteration that down-regulates the expression of the reduced folate carrier (22, 23). Hence, in this study, MDA-MB-231 cells were treated with methotrexate bound to albumin (17, 24, 25), which enters the cells by albumin-mediated endocytosis (25) and circumvents the methotrexate transport deficiency of MDA-MB-231 cells. The other cell lines were treated with free methotrexate. Sixteen hours after treatment with methotrexate or methotrexate-albumin, cells were treated with AICA riboside and, 2 hours later, intracellular ZMP accumulation was measured. After treatment with AICA riboside alone, a measurable increase in intracellular ZMP was found at AICA riboside concentrations starting from 0.250 mmol/L ($P < 0.05$ compared with control; Fig. 1A). On pretreatment with methotrexate-albumin, increases in the levels of ZMP were noticeable at AICA riboside concentrations as low as 0.015 mmol/L. Similar effects were observed in PC-3M-luc-C6 and A-431

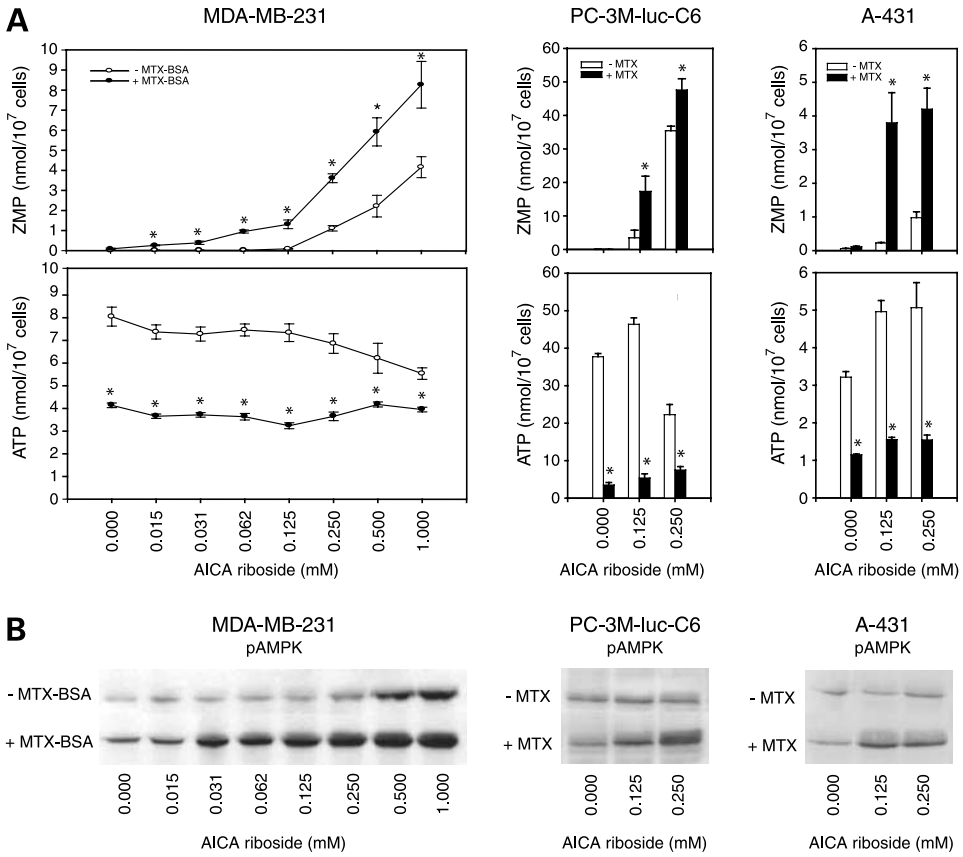

Figure 1. Methotrexate enhances the ability of AICA riboside to activate AMPK by stimulating the accumulation of ZMP and by decreasing the levels of ATP. **A,** measurement of ZMP and ATP. MDA-MB-231 cells were pretreated with methotrexate (*MTX*)-albumin (*MTX-BSA*; 5 μmol/L) or with albumin vehicle for 16 h, whereas PC-3M-luc-C6 and A-431 cells were treated with 5 μmol/L of unbound methotrexate for 16 hours. AICA riboside was added as indicated and, after 2 h of incubation, ZMP and ATP levels were measured using tandem electrospray-mass spectrometry and a luciferase-based assay, respectively. *Points,* mean of triplicate measurements; *bars,* SE. *, $P < 0.05$, significantly different from values of cultures with the same concentration of AICA riboside but without methotrexate. **B,** immunoblot analysis of phosphorylated Thr^{172} AMPKα (*pAMPK*). Cells were pretreated with methotrexate-albumin (5 μmol/L; MDA-MB-231), methotrexate (5 μmol/L; PC-3M-luc-C6 and A-431), or with vehicle for 16 h. AICA riboside was added as indicated. After 3 h of incubation, equal amounts of proteins were subjected to immunoblot analysis with an antiserum against phosphorylated Thr^{172} AMPKα. Total levels of AMPK (irrespective of its phosphorylation status) were not affected (data not shown). Results are representative of three independent experiments.

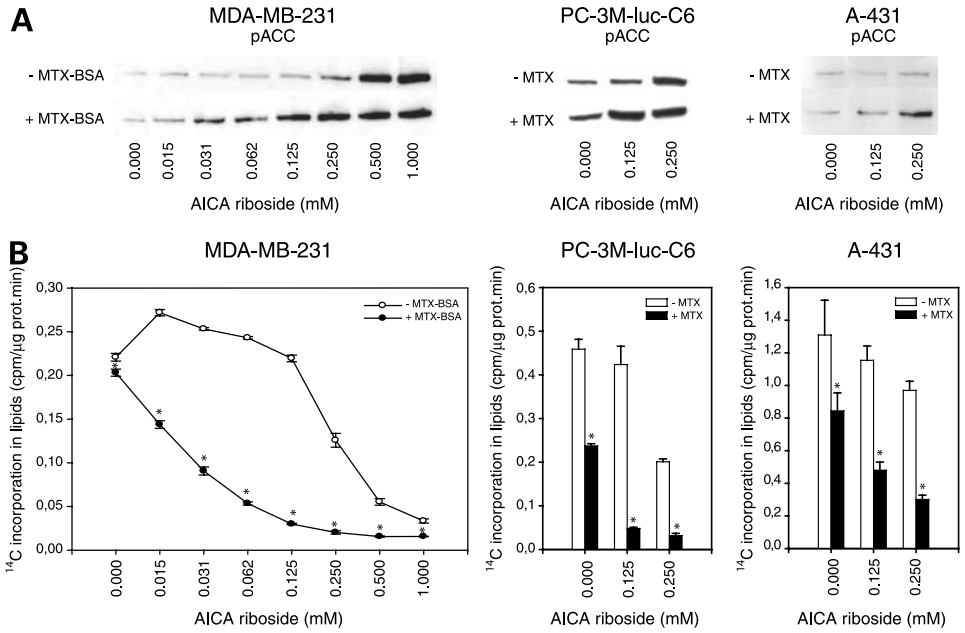

Figure 2. Methotrexate enhances the inhibitory effects of AICA riboside on tumor-associated lipid production. **A,** the same cell extracts used in Fig. 1B were subjected to Western blot analysis with an antiserum against phosphorylated Ser^{79} acetyl-CoA carboxylase (*pACC*). Equal loading of proteins was confirmed by immunoblotting for cytokeratin-18 (data not shown). Results are representative of two independent experiments. **B,** cells were incubated with methotrexate-albumin (5 μmol/L; MDA-MB-231), methotrexate (5 μmol/L; PC-3M-luc-C6 and A-431), or vehicle for 16 h and then treated with different concentrations of AICA riboside. One hour later, ^{14}C-labeled acetate was added. After 4 h of incubation, lipids were extracted and ^{14}C incorporation into lipids was measured. Values were corrected for differences in protein content of the cultures and expressed relative to the values of the untreated cells. *Points* and *columns,* mean of three values; *bars,* SE. *, $P < 0.05$, significantly different from values of cultures with the same concentration of AICA riboside but without methotrexate.

cells where, at an AICA riboside concentration of 0.125 mmol/L, the addition of methotrexate induced a 5-fold increase in the ZMP levels.

As methotrexate-induced inhibition of the *de novo* purine synthesis is expected to decrease the cellular ATP pool (15, 16) and ATP is an intrasteric inhibitor of AMPK (9), we also examined the effect of methotrexate on the levels of ATP. As shown in Fig. 1A, methotrexate caused an overall 2-fold decrease of the levels of ATP in MDA-MB-231 cells, with somewhat less pronounced effects at high concentrations of AICA riboside. In PC-3M-luc-C6 and A-431 cells, methotrexate caused a 5-fold decrease of the ATP levels. Consistent with the increased ZMP levels at low concentrations of AICA riboside and with the fact that

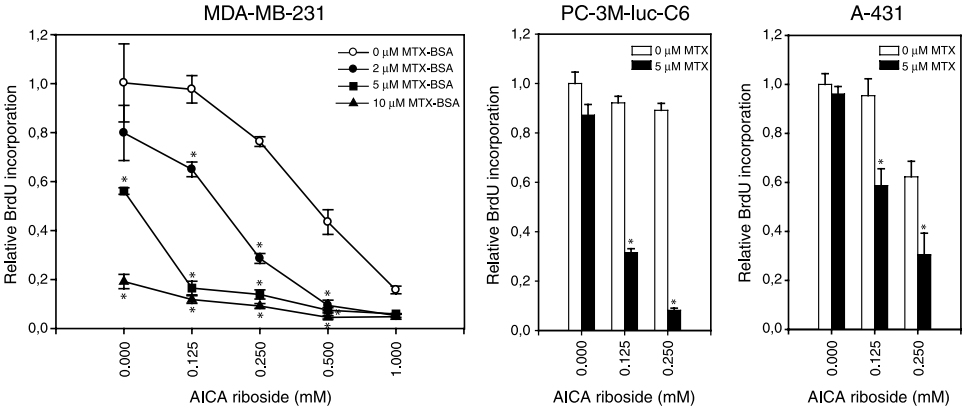

Figure 3. Methotrexate cooperates with AICA riboside to inhibit DNA synthesis. Cells were seeded in 96-well plates at 5×10^3 per well. Two days later, MDA-MB-231 cells were treated with methotrexate-albumin (0, 2, 5, and 10 μmol/L) or with vehicle. PC-3M-luc-C6 and A-431 cells were treated with methotrexate (0 and 5 μmol/L). Four h later, AICA riboside was added. After incubation for 16 h, BrdUrd was added and incorporation into DNA was measured. Representative of two experiments. *Points* and *columns,* mean of quadruplicates from one experiment; *bars,* SE. *, $P < 0.05$, significantly different from values of cultures with the same concentration of AICA riboside but without methotrexate.

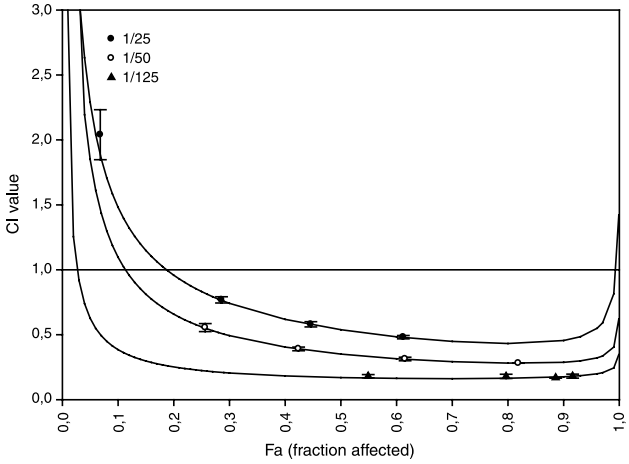

Figure 4. Analysis of combined drug effects shows methotrexate and AICA riboside to act synergistically on proliferation of PC-3M-luc-C6 cells. PC-3M-luc-C6 cells were treated with methotrexate or AICA riboside alone or with a fixed ratio of methotrexate and AICA riboside. The combined effect at three different ratios (1:25, 1:50, and 1:125) was analyzed by CI analysis (19). Experimental CI were plotted against the fractional inhibition (fraction affected; *Fa*) as measured by BrdUrd incorporation. Experimental CIs correspond to 1, 2, 5, and 10 μmol/L methotrexate combined with the concentration of AICA riboside at a fixed ratio as indicated. Representative of three experiments. *Points,* mean of quadruplicates from one experiment; *bars,* SE.

AMPK is more sensitive to activation at lower ATP levels (5, 9), methotrexate-albumin potently increased the ability of AICA riboside to activate AMPK in MDA-MB-231 cells, as shown by Western blot analysis with an antiserum recognizing the Thr^{172}-phosphorylated (and thus active) form of AMPK (Fig. 1B). In PC-3M-luc-C6 and A-431 cells, similar results were obtained using free methotrexate as shown in Fig. 1B. In agreement with the transport deficiencies of methotrexate in MDA-MB-231 cells, free methotrexate did not enhance the effects of AICA riboside on the phosphorylation of MDA-MB-231 cells (data not shown).

Methotrexate Enhances the Inhibitory Effect of AICA Riboside on Tumor-Associated Lipid Production

One of the main targets of AMPK is acetyl-CoA carboxylase, one of the key enzymes involved in fatty acid synthesis and in the regulation of fatty acid oxidation (4, 26). In previous studies, AICA riboside at high concentrations was shown to affect the phosphorylation state of acetyl-CoA carboxylase in MDA-MB-231 cells (1). To examine whether methotrexate enhances these effects, MDA-MB-231 cells were incubated with methotrexate-albumin, with AICA riboside or with a combination of both drugs. As shown in Fig. 2A, phosphorylation of acetyl-CoA carboxylase was observed at lower concentrations of AICA riboside when cells were pretreated with methotrexate-albumin. These effects were paralleled by the inhibition of the incorporation of ^{14}C of ^{14}C-labeled acetate into extractable lipids (Fig. 2B). Treatment of MDA-MB-231 cells with AICA riboside alone resulted in a dose-dependent decrease of lipid production with half-maximal effects at 0.260 mmol/L. In the presence of methotrexate-albumin, effects of AICA riboside on lipid production were half-maximal at 0.025 mmol/L. At 0.125 mmol/L, lipid production was almost completely shut down, reaching values obtained at 1 mmol/L AICA riboside alone. Similar enhancing effects of methotrexate were observed in PC-3M-luc-C6 and A-431 cancer cells (Fig. 2A and B).

Methotrexate Cooperates Synergistically with AICA Riboside to Block DNA Synthesis

Methotrexate is known to potently inhibit DNA synthesis. AICA riboside has also been shown to attenuate DNA synthesis (1). Here, we examined whether cotreatment of cancer cells with both compounds results in stronger effects on DNA synthesis than with each compound individually. To assess the effects on DNA synthesis, the incorporation of the thymidine analogue BrdUrd was measured using an ELISA technique. Treatment of cancer cells with AICA riboside alone caused a potent and dose-dependent reduction of BrdUrd incorporation in all three tested cell

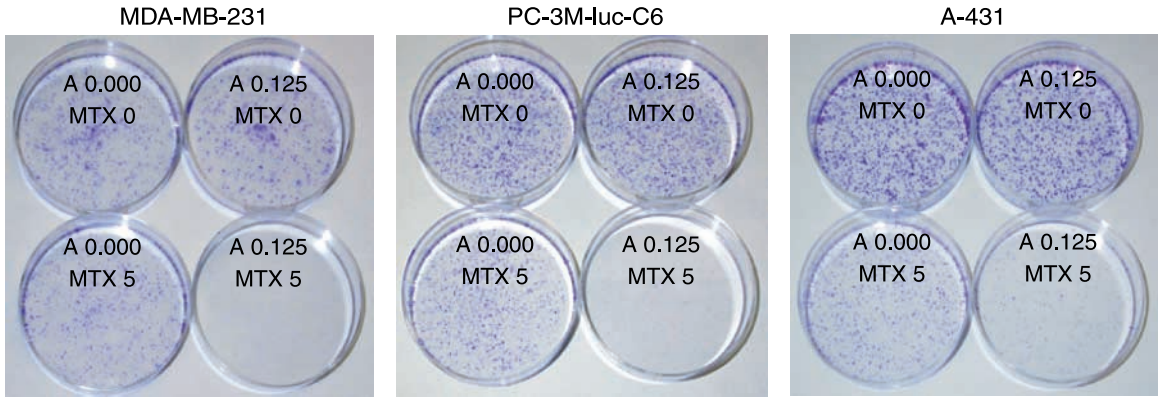

Figure 5. Effect of methotrexate and AICA riboside on colony formation. MDA-MB-231, PC-3M-luc-C6, and A-431 cells were seeded at a density of 5×10^3 per 6-cm dish. The next day, cultures were treated with methotrexate, methotrexate-albumin (5 μmol/L), or vehicle. Four hours later, AICA riboside (0.125 mmol/L) was added. Three days later, medium was changed and treatment was repeated. Eight days after initial treatment, cultures were fixed, stained with a crystal violet solution, and photographed.

lines (Fig. 3). Methotrexate or methotrexate-albumin alone also caused a dose-dependent decrease in BrdUrd incorporation and, importantly, caused a major shift in the dose-response curve of AICA riboside.

To determine whether the inhibitory effects of methotrexate and AICA riboside were synergistic, CI analysis (19) of the effects on DNA synthesis was done on PC-3M-luc-C6 cells. Cells were treated with different concentrations of methotrexate or AICA riboside alone or with a fixed ratio (methotrexate/AICA riboside: 1:25, 1:50, or 1:125) of both drugs simultaneously as shown in Fig. 4. Synergistic effects (CI < 1) were observed for all three tested ratios of methotrexate/AICA riboside. For the combination of 5 μmol/L methotrexate with 0.125 and 0.250 mmol/L AICA riboside that we also used in other experiments, CI indicating synergism (0.3 < CI < 0.7) and strong synergism (0.1 < CI < 0.3), respectively, were observed (20).

Methotrexate Cooperates with AICA Riboside to Block Colony Formation

To assess the effect of drug treatment on the growth of cancer cells, we treated MDA-MB-231, PC-3M-luc-C6, and A-431 cells with AICA riboside in the presence or absence of methotrexate or methotrexate-albumin and assessed the ability of individual cancer cells to form colonies. As shown in Fig. 5, a remarkable concerted effect of both compounds was observed. Whereas 5 μmol/L methotrexate or methotrexate-albumin alone and 0.125 mmol/L AICA riboside alone had little or no effect on colony formation, the combination of both compounds led to a severe reduction both in the size and in the number of colonies.

RNA Interference–Mediated Silencing of ATIC and/or GART in Combination with AICA Riboside Reduces Colony Formation

To confirm that methotrexate sensitizes cancer cells for the effect of AICA riboside by inhibition of enzymes of the *de novo* purine synthesis pathway (ATIC and/or GART), we specifically inhibited these enzymes by the RNA interference technique. MDA-MB-231 and PC-3M-luc-C6 cells were transiently transfected with Stealth siRNA oligonucleotides targeting ATIC and/or GART or with a scrambled oligonucleotide as a negative control. Northern blot analysis showed a marked suppression of ATIC and GART after transfection of PC-3M-luc-C6 cells with respective siRNAs (Fig. 6A–B). As shown in Fig. 6C, RNA interference–mediated silencing of ATIC or GART in the absence of AICA riboside had little or no effects on colony formation. In the presence of exogenous AICA riboside, however, knockdown of ATIC enhanced ZMP accumulation and potently sensitized PC-3M-luc-C6 cancer cells for the inhibiting effect of AICA riboside on colony formation. Despite the fact that exogenous AICA riboside enters the *de novo* purine synthesis pathway downstream of GART, we also observed that inhibition of GART enhanced AICA riboside–induced ZMP accumulation and sensitized cancer cells for the effect of AICA riboside (data not shown). These findings suggest that silencing of GART may have a more complex effect on the *de novo* purine biosynthesis pathway than expected and indicate that methotrexate may sensitize cancer cells for AICA riboside through inhibition of both ATIC and GART. Similar effects were observed in MDA-MB-231 cells (data not shown).

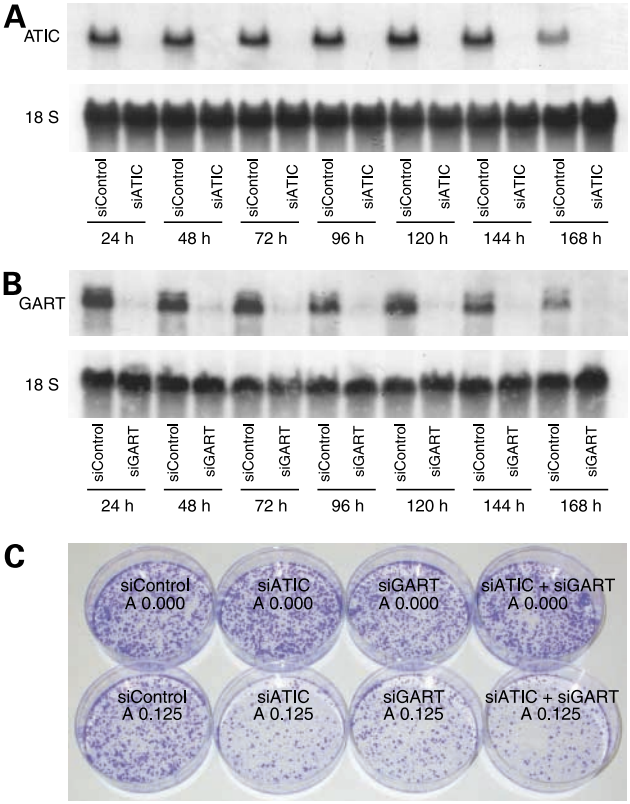

Figure 6. RNA interference–mediated silencing of ATIC and/or GART in combination with AICA riboside reduces colony formation. **A** and **B,** PC-3M-luc-C6 cells were transfected with Stealth siRNAs targeting ATIC (*siATIC*) and/or GART (*siGART*) or with control siRNAs (*siControl*; scrambled nucleotide sequence of ATIC siRNAs). At the indicated time points after transfection, the expression of ATIC (**A**) and GART (**B**) was analyzed by Northern blot analysis. 18S rRNA expression was used as loading control. **C,** 24 h after transfection with Stealth siRNAs, PC-3M-luc-C6 cells were trypsinized and reseeded at a density of 5×10^3 per 6-cm dish. The next day, cultures were treated with AICA riboside (0.125 mmol/L). Three days later, medium was changed and treatment was repeated. The 8-d cultures were fixed, stained with a crystal violet solution, and photographed.

Discussion

The clinical use of antineoplastic agents is often limited by the high doses of compounds that are required to exert effects and by the accompanying dose-related side effects. Cotreatment with multiple chemical compounds that have complementary mechanisms of action or that elicit effects through different antineoplastic pathways often provides interesting avenues toward more effective cancer interventions. Here, we combined two antimetabolic agents that, both in terms of mechanisms of action and in terms of the affected cellular pathways, are complementary. AICA riboside evokes an increase of the intracellular levels of ZMP and through subsequent activation of AMPK leads to

inhibition of major energy-demanding cancer-associated processes, including lipid production, DNA synthesis, and matrix invasion. Methotrexate exerts its antineoplastic effects through inhibition of folate-dependent enzymes, including ATIC, the main enzyme metabolizing ZMP, in the *de novo* purine synthesis pathway. Here, we took advantage of this ability of methotrexate to block the metabolism of ZMP to augment the ZMP levels generated after treatment with exogenous AICA riboside and to decrease simultaneously the levels of ATP, which functions as an inhibitor of AICA riboside–induced activation of AMPK. The net result is a marked sensitization of AMPK for activation by AICA riboside and a major sensitization of the cells toward AICA riboside–induced inhibition of key tumor-associated processes, including lipid production, DNA synthesis, and colony formation. Importantly, this sensitization was already observed at concentrations of compounds that were only marginally effective when used alone and led to synergistic effects. The end result of this cooperative action is that much lower concentrations of each compound are needed to exert antineoplastic effects compared with monotreatment, alleviating several of the limitations related to the high doses required of each compound when given alone. This way, our findings provide new opportunities for both the application of classic antimetabolic chemotherapeutics, such as methotrexate and its derivates, and the exploitation of the energy-sensing machinery as a target for cancer intervention. The recent development of more selective inhibitors of ATIC and GART (27) may improve the efficacy and selectivity of the chemotherapeutic strategy described in this report.

References

1. Swinnen JV, Beckers A, Brusselmans K, et al. Mimicry of a cellular low energy status by AICA riboside-induced ZMP accumulation blocks tumor cell anabolism and suppresses the malignant phenotype. Cancer Res 2005;65:2441 – 8.

2. Xiang X, Saha AK, Wen R, Ruderman N, Luo Z. AMP-activated protein kinase activators can inhibit the growth of prostate cancer cells through multiple mechanisms. Biochem Biophys Res Commun 2004;321:161 – 7.

3. Rattan R, Giri S, Singh AK, Singh I. 5-Aminoimidazole-4-carboxamide-1-β-D-ribofuranoside inhibits cancer cell proliferation *in vitro* and *in vivo* via AMP-activated protein kinase. J Biol Chem 2005;280:39582 – 93.

4. Henin N, Vincent MF, Gruber HE, Van den Berghe G. Inhibition of fatty acid and cholesterol synthesis by stimulation of AMP-activated protein kinase. FASEB J 1995;9:541 – 6.

5. Corton JM, Gillespie JG, Hawley SA, Hardie DG. 5-aminoimidazole-4-carboxamide ribonucleoside. A specific method for activating AMP-activated protein kinase in intact cells? Eur J Biochem 1995;229:558 – 65.

6. Carling D. The AMP-activated protein kinase cascade: a unifying system for energy control. Trends Biochem Sci 2004;29:18 – 24.

7. Hardie DG. Minireview: the AMP-activated protein kinase cascade: the key sensor of cellular energy status. Endocrinology 2003;144:5179 – 83.

8. Sabina RL, Patterson D, Holmes EW. 5-amino-4-imidazolecarboxamide riboside (Z-riboside) metabolism in eukaryotic cells. J Biol Chem 1985; 260:6107 – 14.

9. Adams J, Chen ZP, Van Denderen BJ, et al. Intrasteric control of AMPK via the γ1 subunit AMP allosteric regulatory site. Protein Sci 2004;13: 155 – 65.

10. Schilsky RL. Methotrexate: an effective agent for treating cancer and building careers. The polyglutamate era. Stem Cells 1996;14:29 – 32.

11. Allegra CJ, Hoang K, Yeh GC, Drake JC, Baram J. Evidence for direct inhibition of *de novo* purine synthesis in human MCF-7 breast cells as a principal mode of metabolic inhibition by methotrexate. J Biol Chem 1987; 262:13520 – 6.

12. Costi MP, Ferrari S. Update on antifolate drugs targets. Curr Drug Targets 2001;2:135 – 66.

13. Allegra CJ, Fine RL, Drake JC, Chabner BA. The effect of methotrexate on intracellular folate pools in human MCF-7 breast cancer cells. Evidence for direct inhibition of purine synthesis. J Biol Chem 1986; 261:6478 – 85.

14. Allegra CJ, Drake JC, Jolivet J, Chabner BA. Inhibition of phosphoribosylaminoimidazolecarboxamide transformylase by methotrexate and dihydrofolic acid polyglutamates. Proc Natl Acad Sci U S A 1985;82: 4881 – 5.

15. Budzik GP, Colletti LM, Faltynek CR. Effects of methotrexate on nucleotide pools in normal human T cells and the CEM T cell line. Life Sci 2000;66:2297 – 307.

16. Kaminskas E. Effects of methotrexate on ribonucleotide pools in growing and in growth-arrested tumor cells and antagonism by RNA synthesis inhibitors. J Biol Chem 1982;257:4279 – 84.

17. Stehle G, Sinn H, Wunder A, et al. The loading rate determines tumor targeting properties of methotrexate-albumin conjugates in rats. Anticancer Drugs 1997;8:677 – 85.

18. Swinnen JV, Van Veldhoven PP, Esquenet M, Heyns W, Verhoeven G. Androgens markedly stimulate the accumulation of neutral lipids in the human prostatic adenocarcinoma cell line LNCaP. Endocrinology 1996; 137:4468 – 74.

19. Chou TC, Talalay P. Quantitative analysis of dose-effect relationships: the combined effects of multiple drugs or enzyme inhibitors. Adv Enzyme Regul 1984;22:27 – 55.

20. Reynolds CP, Maurer BJ. Evaluating response to antineoplastic drug combinations in tissue culture models. Methods Mol Med 2005;110: 173 – 83.

21. Swinnen JV, Ulrix W, Heyns W, Verhoeven G. Coordinate regulation of lipogenic gene expression by androgens: evidence for a cascade mechanism involving sterol regulatory element binding proteins. Proc Natl Acad Sci U S A 1997;94:12975 – 80.

22. Pinard MF, Jolivet J, Ratnam M, et al. Functional aspects of membrane folate receptors in human breast cancer cells with transport-related resistance to methotrexate. Cancer Chemother Pharmacol 1996; 38:281 – 8.

23. Worm J, Kirkin AF, Dzhandzhugazyan KN, Guldberg P. Methylation-dependent silencing of the reduced folate carrier gene in inherently methotrexate-resistant human breast cancer cells. J Biol Chem 2001;276: 39990 – 40000.

24. Burger AM, Hartung G, Stehle G, Sinn H, Fiebig HH. Pre-clinical evaluation of a methotrexate-albumin conjugate (MTX-HSA) in human tumor xenografts *in vivo*. Int J Cancer 2001;92:718 – 24.

25. Wosikowski K, Biedermann E, Rattel B, et al. *In vitro* and *in vivo* antitumor activity of methotrexate conjugated to human serum albumin in human cancer cells. Clin Cancer Res 2003;9:1917 – 26.

26. Carling D, Zammit VA, Hardie DG. A common bicyclic protein kinase cascade inactivates the regulatory enzymes of fatty acid and cholesterol biosynthesis. FEBS Lett 1987;223:217 – 22.

27. Cheong CG, Wolan DW, Greasley SE, Horton PA, Bearsley GP, Wilson IA. Crystal structures of human bifunctional enzyme aminoimidazole carboxamide ribonucleotide tranformylase/IMP cyclohydrolase complex with potent sulfonyl-containing antifolates. J Biol Chem 2004;279: 18034 – 45.